CNWRA *A center of excellence in earth sciences and engineering*

A Division of Southwest Research Institute™
6220 Culebra Road • San Antonio, Texas, U.S.A. 78228-5166
(210) 522-5160 • Fax (210) 522-5155

June 3, 2002
Contract No. NRC–02–97–009
Account No. 20.01402.571

U.S. Nuclear Regulatory Commission
ATTN: Mrs. Deborah A. DeMarco
Two White Flint North
11545 Rockville Pike
Mail Stop T8 A23
Washington, DC 20555

Subject: Programmatic review of the paper titled "Effect of Palladium on the Corrosion Behavior of Titanium" for submission to the Journal Corrosion Science

Dear Mrs. DeMarco:

Attached is the subject paper to be submitted to the Corrosion Journal. The paper describes the results from a series of experiments examining the localized and general corrosion behavior of Titanium Grade 7, the proposed material for the drip shield. Information in this paper has been presented previously in IM 01402.571.170 titled "Effect of Environment on the Corrosion of Waste Package and Drip Shield Materials" (CNWRA 2001-003) and the NACE Corrosion 2001 Conference paper "Effect of Palladium on the Localized and Passive Dissolution of Titanium" that have been previously reviewed and approved by the NRC staff.

Please contact Sean Brossia at (210) 522-5797 or Gustavo Cragnolino (210) 522-5539 if you have any questions regarding this paper.

Sincerely yours,

Budhi Sagar
Technical Director

BS:SB:jg

Enclosure

cc:	J. Linehan	B. Leslie	J. Andersen	W. Patrick	L. Yang
	B. Meehan	S. Wastler	J. Thomas	B. Sagar	D. Dunn
	E. Whitt	D. Brooks	T. Essig	CNWRA Dirs. (cvr ltr only)	O. Pensado
	W. Reamer	T. McCartin	A. Henry	CNWRA EMs (cvr ltr only)	Y.-M. Pan
	J. Greeves	T. Ahn	J. Schlueter	G. Cragnolino	P. Maldonado
	K. Stablein	T. Bloomer	A. Campbell	S. Brossia	T. Nagy (contracts)

Washington Office • Twinbrook Metro Plaza #210
12300 Twinbrook Parkway • Rockville, Maryland 20852-1606

Effect of Palladium on the Corrosion Behavior of Titanium

C.S. Brossia and G.A. Cragnolino

Center for Nuclear Waste Regulatory Analyses

Southwest Research Institute

6220 Culebra Road

San Antonio, TX 78238

ABSTRACT

The effects of palladium (Pd) additions on the localized and uniform corrosion of titanium (Ti) were examined by comparing the corrosion behavior of Ti Grade 2 (UNS R50400) to that of Pd-bearing Ti Grade 7 (UNS R52400). Pd additions were found to increase the pitting (E_{pit}) and repassivation (E_{rp}) potentials such that E_{pit} for Ti Grade 2 was significantly lower than E_{rp} for Grade 7 in chloride (Cl^-) solutions. The effect of Pd on Ti can be explained through the effects Pd has on the hydrogen evolution reaction. Though Pd additions did significantly affect the localized corrosion resistance of Ti, Pd did not appear to influence the passive corrosion rate nor did it mitigate the deleterious effects of fluoride (F^-). Fluoride was found to dramatically increase the measured corrosion current above a critical concentration of about 0.5 mM.

Keywords: Titanium, palladium, fluoride, hydrogen evolution, pitting corrosion, crevice corrosion, passive corrosion

INTRODUCTION

The U.S. Department of Energy (DOE) is responsible for the permanent disposal of high-

level nuclear waste (HLW) generated in the United States. DOE's current plans for HLW management call for the emplacement of the waste into dual container waste packages constructed from an inner container of Type 316 Nuclear Grade (similar to Type 316LN, UNS S31653) and an outer container of Alloy 22 (UNS N06022). The safety strategy currently proposed by the DOE relies on several key attributes of the disposal system to maintain public health and safety, one of which is long waste package lifetime.[1] In an effort to increase waste package lifetimes, the DOE is considering the use of a drip shield to divert incoming water away from the container thereby minimizing the quantity of water that may come in contact with the container.[2] The primary material being considered by the DOE for construction of the drip shield is Pd–bearing Ti alloys [*e.g.*, Ti Grades 7 and 16 (no UNS designation)].

Ti–Pd alloys are α–Ti alloys and, as with all Ti alloys, are known to exhibit excellent corrosion resistance in many aqueous environments as a result of the spontaneous formation of a protective TiO_2 passive film. It has been generally accepted that Ti alloys tend to be highly resistant to pitting corrosion in chloride (Cl^-) solutions, but can more readily undergo crevice corrosion. Based on the prevailing conditions anticipated at the proposed Yucca Mountain repository (i.e., slightly oxidizing), several reviews have been generated describing the likely corrosion failure modes that may be encountered.[3,4] Though a range of possible water chemistries may develop as a result of groundwater-rock interactions and possible concentration of dissolved species resulting from water evaporation, the primary corrosion modes identified include aqueous corrosion under condensed vapor conditions, aqueous corrosion (including general and localized corrosion, stress corrosion cracking and hydrogen embrittlement, and galvanic interactions with other materials) resulting from dripping water onto the drip shield or adsorption of water at hygroscopic salts. In any

event, these solutions are generally thought to contain chlorides, nitrates, sulfates, and fluorides and may have pH values ranging from near neutral to alkaline. Previous work by the authors[5,6] indicated that Ti–Pd alloys were immune to crevice corrosion in oxidizing Cl^- solutions in line with the reported performance of Pd–bearing Ti alloys.[7,8] It was speculated that the lack of crevice corrosion was a consequence of the absence of an active/passive transition for Ti Grade 7 even in highly aggressive solutions. To further evaluate this possibility, testing of Ti Grade 2 was initiated to serve as a basis for comparison to Grade 7, as more information on the corrosion behavior of Grade 2 (and other similar Ti alloys) has been published than for Pd–bearing Ti alloys, and as a way to better understand the role of Pd on the localized and passive corrosion of Ti alloys under potential repository conditions.

EXPERIMENTAL APPROACH

All tests on Ti Grade 7 were performed using specimens machined from a single 2.5 cm thick plate. Ti Grade 2 specimens were either machined from a 0.95 cm thick plate for crevice specimens or from a 0.95 cm diameter rod for cylindrical specimens. The compositions for each material are shown in Table 1. Specimens were machined in the form of cylinders 6.3 mm in diameter and 48.6 mm in length or as standard crevice specimens in the form of blocks with dimensions of 19 × 19 × 12 mm (length × width × thickness) with an 8 mm hole through the thickness to facilitate attachment of the crevice former. For crevice specimens, a serrated polytetrafluoroethylene (PTFE) crevice former having 12 crevice feet was used for one side and a solid PTFE block was used for the other. The crevice formers were pressed against the flat portion of the specimen at a torque of 0.28 N·m. All specimens were wet polished to a 600 grit finish and ultrasonically cleaned in acetone and water

prior to testing. All test solutions were made from reagent grade sodium or lithium salts, reagent grade acids, and 18 MΩ·cm water. Unless intentionally acidified, the solution pH was found to be near neutral for all conditions studied. After the bulk solution was made, the solution was introduced into the test cell, purged with high purity N_2, and heated to the desired temperature prior to introduction of the specimen to the cell. All tests used a Pt-coated Nb mesh or graphite rod counter electrode and a saturated calomel electrode (SCE) as a reference, introduced into the cell through a salt bridge/Luggin probe to maintain the reference electrode at room temperature.

Both cyclic potentiodynamic and potentiostatic polarization tests were performed. Cyclic polarization tests were performed at a scan rate of 0.167 mV/s and were reversed at a current density of 5 mA/cm^2, with the exception of tests conducted in F^- solutions and solutions simulating the solution chemistry of a propagating crevice, in which case the scans were terminated at 1.0 V_{SCE}. Potentiostatic tests were performed to examine the effects of environmental and electrochemical variables on passive dissolution and to examine the effects of long-term polarization on the possible initiation of localized corrosion.

EXPERIMENTAL RESULTS

Figure 1 summarizes the effects of chloride concentration on E_{pit} and E_{rp} determined from cyclic potentiodynamic polarization (CPP) experiments performed at 95 °C for Ti Grades 2 and 7. The typical attack morphology observed after polarization is shown in Figure 2. Note that localized corrosion is evident; however, the morphology of the attack is extremely irregular. Furthermore, under no conditions was attack observed under the crevice former during CPP testing, but rather all attack was observed on the boldly exposed surfaces of the specimens. As a result, the breakdown and repassivation potentials are not associated with crevice corrosion despite the use of creviced

specimens. Both Ti Grades 2 and 7 exhibited a dependence of E_{pit} and E_{rp} on Cl^- concentration according to Eq. 1,

$$E_{crit} = E^0_{crit} - B_{crit} \log[Cl^-] \quad (1)$$

where E_{crit} is the critical potential (either E_{pit} or E_{rp}), E^0_{crit} is the critical potential at 1 M chloride concentration, and B is the slope of the dependence of E_{crit} on the log of the chloride concentration. The values for E^0_{crit} and B are summarized in Table 2. In general, the primary difference between Ti Grade 2 and Grade 7 was E^0_{crit} (i.e., the curve offset) with only slight differences observed in the slope of the curves. For example, E^0_{rp} and B_{rp} for Grade 7 were 5.61 V_{SCE} and 1.02 V/pCl^-, whereas for Grade 2 they were 0.72 V_{SCE} and 1.06 V/pCl^-. Furthermore, E_{rp} for Grade 7 was observed to be greater than E_{pit} for Grade 2. Except at low [Cl^-] ($\leq$ 0.1 M), this difference was on the order of 4.5 V. At lower [Cl^-], Grade 2 exhibited a transition to much higher critical potentials, but these potentials were still less than those measured for Grade 7.

As no crevice corrosion of Grade 2 was observed in the CPP tests and Grade 2 is known to be susceptible to crevice corrosion,[9,10] a series of potentiostatic experiments was conducted. The potential chosen was 0 V_{SCE}, which was found to be a readily achievable open circuit potential (–0.3 to 0 V_{SCE}) under air-saturated conditions[6]. If no crevice corrosion initiated under the conditions studied, then the tests were used as a measurement of the long-term passive corrosion rate. Figure 3 shows the results of potentiostatic holds in deaerated solutions at 95 °C. Crevice corrosion initiated on Grade 2 held at 0 V_{SCE} in 5 M Cl^- after an induction time of ~ 32 hr. This induction time was measured from the start of the experiment to the point at which the current density exceeded 1 $\mu A/cm^2$ and was observed to continue increasing. The morphology of the crevice attack is shown

in Figure 4. In this case, attack was general in nature and located exclusively underneath the crevice former. It is also evident on observation of the specimen that crevice corrosion did not initiate as pits that coalesced together. Also shown in Figure 3 are the passive dissolution rates for Grade 2 in 1 M Cl^- and Grade 7 in 5 M Cl^-. The inset figure shows an expanded view of the current axis. For both Grade 2 in 1 M Cl^- and Grade 7 in 5 M Cl^- the measured currents were quite low, averaging 0.099 and 0.074 $\mu A/cm^2$ respectively over the nearly 1200 hr of the experiment. It should also be noted that on occasion the measured net current became cathodic.

Because crevice corrosion was observed in Ti Grade 2 in a relatively short time (32 hr) in 5 M Cl^- and Ti Grade 7 did not experience crevice corrosion under similar conditions (at least up to ~ 1200 hr), the cathodic and anodic polarization behaviors of Ti Grades 2 and 7 were examined in a simulated crevice solution (deaerated, 5 M Cl^-, 0.1 M HCl, 95 °C). Figure 5 shows the cathodic polarization curves for Ti Grades 2 and 7 with Ti Grade 7 exhibiting a higher open circuit potential. During cathodic polarization, evolution of gas, assumed to be H_2, was observed. For both materials, an activation controlled region was observed that was then followed by a mass transport limited region. The cathodic Tafel slope observed for Ti Grade 2 was –100 mV/decade. Ti Grade 7 exhibited a cathodic Tafel slope of –27 mV/decade at low overpotenentials that transitioned to a slope of –138 mV/decade at higher cathodic overpotentials. Anodic polarization of Ti Grade 2 (Figure 6) resulted in the observation of an active/passive transition, with a peak current of nearly $8x10^{-4}$ A/cm^2 prior to decreasing to ~ $2x10^{-5}$ A/cm^2. Anodic polarization of Ti Grade 7 exhibited essentially passive behavior at all potentials above the corrosion potential. Furthermore, there was little difference in the observed passive current for either material, but the passive current density did decrease with increasing polarization. Post-test examination of the specimens revealed that they had

not experienced localized corrosion.

In addition to the likely presence of Cl^- ions in the water contacting the drip shield, the possibility exists for free F^- ions to also be present as it is known to exist at low concentrations (~ 0.1 mM) in the local groundwater at the proposed repository site at Yucca Mountain (YM), NV and has been shown to reach higher concentrations on repeated dryout and rewetting.[3] Thus, the effect of F^- on the polarization of Ti was examined. Shown in Figure 7 are two polarization curves for non-creviced Ti Grade 7 specimens comparing the anodic behavior observed in 1 M NaCl and 1 M NaF + 1 M NaCl solutions. As can be seen, Ti Grade 7 exhibited a considerably lower open circuit potential on the addition of F^- and a pseudo active/passive transition with a subsequent potential independent current region with current densities considerably higher than those typically encountered during passive dissolution (10^{-3} to 10^{-1} as compared to ~ 10^{-6} A/cm^2). It is also interesting to note that a small area of passivity just noble of the open circuit potential was observed in many of the $Cl^- + F^-$ solutions,[6] prior to a sharp increase in the current (similar to what is observed during localized corrosion) which then decreased after reaching a critical current density. Post-test examination of the specimens revealed extensive attack, but the attack was generalized in nature.

Using a reasonably achievable open circuit potential (0 V_{SCE}) as a reference point, the dissolution rate observed during potentiostatic testing as a function of [F^-] was examined over extended periods of time. Shown in Figure 8 is the current density measured from potentiostatic tests at 0 V_{SCE} as a function of [F^-] and time for Ti Grade 7 in 1 M chloride solutions. Ti Grade 2 was not evaluated as previous results indicated that little difference in the measured current for Ti Grades 2 and 7 were observed during CPP and short-term potentiostatic testing.[11] As can be seen, the measured current increases significantly with increasing [F^-] above a concentration of 0.5 mM.

Increases in [F^-] from 0.5 mM to 10 mM caused an increase in the dissolution rate by over two orders of magnitude. Further increases in [F^-] beyond 10 mM did not tend to result in higher observed currents. To more clearly illustrate the effects of [F^-] on the measured current, the current measured at the end of the experiment as a function of [F^-] is replotted in Figure 9 in which a linear relationship between the log of the current and the log of [F^-] up to ~ 3 mM is observed followed by a plateau in the measured current. Because other anions may be present in the prevailing groundwater in the vicinity of the proposed repository, the effects on the current in the presence of fluoride were also examined. Figure 10 illustrates that the presence of sulfate and nitrate, even at relatively high concentrations, did not substantially influence the measured currents in the presence of fluoride for Ti Grade 7. For example, the currents measured in 1 M Cl^- + 0.1 M F^- with and without 0.55 M NO_3^- + 0.92 M SO_4^{2-} are essentially indistinguishable at 40 – 70 $\mu A/cm^2$.

DISCUSSION

The objective of this work was to examine the role of Pd on the localized and passive dissolution of Ti alloys to gain a better understanding of how Ti-Pd alloys would behave in the proposed HLW repository at YM and to examine the possible detrimental effects of F^-. To accomplish this, a series of CPP tests was used to establish the differences between the materials in terms of pitting corrosion resistance in Cl^- solutions and differences in dissolution rate in Cl^- + F^- solutions. These tests were augmented through the use of longer-term potentiostatic polarization measurements to examine crevice corrosion susceptibility and to measure passive corrosion rates. The results are discussed in two sections: localized corrosion and uniform corrosion.

Localized Corrosion

Based on the results obtained from CPP tests, it is clear that E_{pit} and E_{rp} for Ti Grades 2 and 7 are dependent on the chloride concentration, following the well established decrease with the logarithm of chloride concentration shown in Eq. 1. In the present work, the slope, B, was greater than 1.3 V/pCl$^-$ for both Ti alloys for a [Cl$^-$] range of 0.1 to 10 M at 95 °C. These values are considerably larger than those observed by Beck[12] of 0.11 V/pBr$^-$ for Ti alloys in bromide solutions and by Koizumi and Furuya[13] in chloride solutions at 200 °C (0.1 V/pCl$^-$). It is speculated that the large change in the E_{rp} at low [Cl$^-$] may be the result of E_{rp} increasing sufficiently to enable changes in the nature and/or structure of the oxide film to take place at higher potentials. This in turn results in higher potentials being necessary to induce localized corrosion. It should be noted, however, that little has been published in the area of the effects of [Cl$^-$] on E_{pit} and E_{rp} compared to the effects of [Br$^-$] and temperature, especially with respect to Pd–bearing Ti alloys. E_{rp} followed a similar relationship to [Cl$^-$], but the slope of the dependence on chloride concentration was lower (slightly larger than 1.0 V/pCl$^-$). In no cases, however, was attack observed under the crevice former with all attack being located on the boldly exposed surfaces of the specimen during cyclic potentiodynamic polarization testing. The beneficial effects of Pd on E_{pit} and E_{rp} observed in the present work are in contrast to results presented by Posey and Bohlmann[14] and summarized by Schutz.[15] These authors noted little or no effect of Pd on pitting behavior and focused much of their efforts with respect to Pd on its beneficial influence on crevice corrosion resistance. The reasons for the differences between the present work and the reported observations in the literature are unclear, but a possible mechanism explaining the role of Pd on improving pitting resistance is provided in subsequent paragraphs.

Previous results[6] indicated that a corrosion potential (E_{corr}) on the order of 0 V_{SCE} is attainable in air-saturated solutions (see Figure 11), which is considerably below the repassivation potentials observed for Ti Grade 7 and is still below those measured for Ti Grade 2 except at very high [Cl^-] (~ 5 M) at 95 °C. Furthermore, it seems unlikely that potentials outside the region of water stability are possible. The exception to this would be the possible formation of hydrogen peroxide (H_2O_2) through radiolysis. Neglecting the well known complexation ability of peroxide with Ti for the moment,[16] addition of peroxide would not likely result in E_{corr} exceeding the repassivation potential of Ti Grade 7, except in highly concentrated H_2O_2 solutions at low pH. Ti Grade 2 could experience pitting at potentials within the stability region of water at [Cl^-] higher than about 0.5 M, but again the E_{rp} predicted from these measurements would be considerably higher than the open circuit potentials measured, and another source of oxidants (beyond O_2) would likely be needed for pitting to occur.

Though it seems that localized corrosion of Ti Grades 2 and 7 only occurs at high overpotentials in chloride solutions, it was also observed that no corrosion occurs under the PTFE crevice former. This seemed to be a surprising result given that Ti alloys have historically been considered more susceptible to crevice corrosion than to pitting corrosion. To evaluate this further, potentiostatic crevice experiments were conducted at an applied potential of 0 V_{SCE}. Ti Grade 2 experienced crevice corrosion after an incubation time of 32 hr in 5 M Cl^-, whereas Ti Grade 7 remained immune to crevice corrosion under the same conditions for at least 1200 hr (Figure 3). If one assumes the explanation put forth by Beck[12] that crevice and pitting corrosion of Ti alloys do not operate via the same mechanism (i.e., crevice corrosion does not initiate through the coalescence of individual pits inside the crevice) and that crevice corrosion occurs with Ti dissolving in the Ti^{3+}

state and pitting occurs with Ti dissolving in the Ti^{4+} state, then the role of Pd on both pitting and crevice corrosion can be explained by coupling the general pitting model put forth by Galvele[17] with the pitting model for Ti put forth by Beck[12] and Cotton.[18]

Galvele's model[17] for pitting involves the localized acidification at the corrosion site, in this case through Eq. 2,

$$Ti + 2H_2O \rightarrow TiO_2 + 4H^+ + 4e^- \quad (2)$$

such that the product of the metal dissolution rate, i, and the diffusion distance, x, exceed a critical value (for most materials this seems to be 10^{-6}A/cm). In Galvele's model, Cl^- acts to accelerate the metal dissolution reaction, and E_{crit} is the overpotential needed to drive the metal dissolution reaction such that sufficient hydrolysis occurs and the local pH drop results. The H^+ ions that are produced according to Eq. 2 can, in addition to lowering the local pH, also diffuse away into the bulk environment, be absorbed by the metal lattice, or be evolved as H_2 gas. Pd is a known catalyst for the hydrogen evolution reaction (HER), with a reported exchange current density (i_0) of 10^{-3} A/cm^2 compared to $6x10^{-9}$ A/cm^2 for Ti.[19] Thus, it would be reasonable to assume that i_0 for HER would be greater on Ti Grade 7 than on Grade 2. Furthermore, Pd has a high affinity for H, such that a considerable fraction of H can be absorbed into the Pd lattice (up to $PdH_{0.6}$).[20] Thus, one could argue that the overpotential needed to achieve the critical pH for sustained pit growth on Ti Grade 7 would be greater than on Ti Grade 2 because of the catalytic effect Pd has on HER and increasing H_{abs}, thereby decreasing the effective H^+ ion concentration. This would translate into a higher E_{pit} and E_{rp} as was observed.

Similarly, the increase in i_0 promoted by the Pd addition could render Ti Grade 7 effectively

immune to crevice corrosion.[7,8] For example, Satoh et al.,[7] observed no initiation of crevice corrosion on Ti Grade 7 in boiling 20 % NaCl solutions at pH 4 after 720 h of exposure and in boiling 42 % $MgCl_2$ solutions after 240 h. In contrast, CP Ti (similar to Grade 2) was observed to suffer from severe crevice corrosion in 92 and 15 h under identical conditions. Similarly, Schutz and Xiao[8] did not observe crevice corrosion in Ti Grade 7 after 30 d exposure in 20% NaCl at pH 2 and 260 °C nor in boiling 10 % $FeCl_3$ solutions (102 °C). If one assumes that Pd will not influence the anodic dissolution behavior of Ti and will only influence the cathodic reaction kinetics, then one would expect to observe an increase in the open circuit potential for Ti Grade 7 compared to Grade 2 in a simulated crevice solution. As shown in Figure 6, this is indeed the case. Note that little difference was in fact observed in the passive region of the polarization curves lending credence to the argument that the main role of Pd is through alteration of the cathodic kinetics as originally proposed by Tomoshov et al.[21] This is further brought out by consideration of the cathodic polarization curves for Ti Grades 2 and 7 (Figure 5). Ti Grade 2 exhibited a cathodic Tafel slope of –100 mV/decade with Ti Grade 7 exhibiting a cathodic Tafel slope of –27 mV/decade at low overpotentials and –138 mV/decade at high overpotentials. Though a detailed study of the HER mechanism on each material was not conducted[a], based on these Tafel slopes and the relationship between the Tafel slope, b, and the transfer coefficient, α, shown in Eq. 3,

$$b = \frac{2.303RT}{\alpha F} \tag{3}$$

[a]To conclusively confirm the HER mechanisms, one would still need to know the stoichiometric number (the number of times the rate determining step takes place each time the reaction sequence occurs once), the reaction order (the dependence of reaction rate on $[H^+]$), and the dependence of H surface coverage on applied potential.

where R is the Universal Gas constant, T is temperature and F is Faraday's constant, some conclusions can be drawn. First, the HER can be broken down into the reaction steps shown in Eq. 4–6,

$$H^+ + e^- \rightarrow H_{ads} \quad (4)$$

$$H_{ads} + H_{ads} \rightarrow H_2 \quad (5)$$

$$H^+ + e^- + H_{ads} \rightarrow H_2 \quad (6)$$

where these represent the discharge, recombination, and electrodic desorption reaction steps. The values of α for each of the reaction steps are 0.5, 2.0, and 1.5 at low H coverage (θ_H)[19] resulting in Tafel slopes (at 95 °C) of –146, –36.5, and –48.7 mV/decade. In the present case then, the likely rate determining step (rds) on Ti Grade 2 is the discharge reaction step (–100 vs. –146 mV/decade) and on Ti Grade 7 at low overpotentials the rds is likely recombination (–27 vs –36.5 mV/decade). At higher overpotentials, it seems likely that the Pd addition to Ti acts in similar fashion as Pt in that as θ_H approaches unity the rds changes to electrodic desorption. At high θ_H, α for electrodic desorption is 0.5[20] which results in a Tafel slope of –146 in comparison to the –138 mV/decade observed here. This conclusion is in agreement with the mechanisms for HER proposed by Fukuzuka et al.[22] for Ti Grade 2 (rds = discharge) but does not agree with their mechanism for Grade 7 (rds = electrodic desorption at low θ_H). This difference in reaction mechanisms is likely a result of the difference in environments examined between Fukuzuka et al.[22] (2% HCl at 70 °C) and the present case. Thus, it appears that Pd acts to increase i_0 and decrease the cathodic Tafel slope (*e.g.*, lower overpotential needed to achieve similar reaction rates) such that the cathodic reaction line no

longer intercepts the anodic dissolution line below the active/passive transition but intersects in the passive range. The consequence of this is that IR drop in the crevice on Ti Grade 2 puts a portion of the crevice in the active nose and rapid dissolution occurs. In Ti Grade 7, IR drop into the crevice does not significantly increase the dissolution rate, and eventually the interior of the crevice will be cathodic and generate H_2 gas or will lead to increased concentrations of H_{abs} in the metal lattice. If Pd accumulates on the metal surface as dissolution proceeds, as has been reported,[21,23-25] then the cathodic reaction kinetics could be further enhanced (e.g., i_0 may increase further) resulting in an additional increase in the open circuit potential and thereby causing the disappearance of the slight active/passive transition observed in the present case.

The explanation given thus far would account for the differences in the crevice corrosion behavior of the materials and explains the relative positions of the critical potentials for pitting corrosion. It does not, however, account for the observation that pitting occurred only on the boldly exposed surfaces and did not occur under the crevice former. If one neglects the argument by Beck[12] that crevice corrosion and pitting corrosion of Ti occur by different mechanisms and focus solely on the model put forth by Galvele[17], the presence of the crevice former should assist in the stabilization of pits as the diffusion length is increased. This would then imply a lower metal dissolution rate is needed and thereby decrease the potential needed to achieve localized corrosion. Thus, one would expect $E_{crev} < E_{pit}$, as is seen with stainless steels and Ni-based alloys.[4] By expanding on the role of Cl^- beyond that assumed by Galvele's model to that proposed by Beck[12] and Cotton[18], Cl^- migration and adsorption at the pit embryo may be a critical step that is partially hindered by the presence of the crevice former by making the diffusion path longer. Thus, there may be a combined effect of local acidification coupled with Cl^- migration and adsorption such that the

presence of a crevice aids the former but hinders the latter such that pitting cannot nucleate and grow under the crevice unless sufficient time is allowed. To examine this further, a series of potentiostatic experiments were carried out using creviced Ti Grade 2 and 7 specimens in 1 M NaCl at relatively high potentials ($E_{applied} > E_{rp}$). After polarization for a period ranging from 24 – 28 hours, the specimens were then removed and examined. It was noted that corrosion attack was prominent on the boldly exposed surfaces (similar to that noted after cyclic potentiodynamic polarization testing) but some attack was also noted within the creviced region as well (Figure 12). Thus, it appears that for pitting and crevice corrosion of Ti a combination of necessary reaction steps involving both Cl^- migration and a pH drop are needed and that for pitting these reaction steps are more readily achievable.

In any event, based on the results reported by Beck[12] and the observation in the present work that crevice corrosion does not initiate by the coalescence of pits, as shown in Figure 4, indications are that crevice corrosion and pitting corrosion of Ti alloys occur by different mechanisms, which is contrary to the case for many engineering materials.

Uniform Corrosion

In addition to Cl^-, another environmental variable to consider with respect to the corrosion behavior of Ti in the proposed repository is the presence of F^- in the local groundwater chemistry that has been observed to approach levels as high as 0.2 M during repeated evaporation/rewetting cycles.[3] Although it is known that F^- acts as a complexant for Ti, the typical concentration ranges that have been examined have been generally in the mM range.[26,27] In addition, there is little information on the effects of Pd on the corrosion behavior of Ti in the presence of F^-. Thus, the possibility that Pd may be beneficial for passive corrosion and corrosion in the presence of F^- was

investigated. Uniform, passive corrosion was observed in Cl^- only solutions, whereas much more rapid uniform corrosion was observed in the presence of $Cl^- + F^-$. If localized corrosion in the form of either pitting or crevice corrosion does not occur, then the next most likely corrosion mode would be uniform passive dissolution.

The passive corrosion rates of both Ti Grade 2 and 7 were quite comparable under the conditions studied here. Previous work demonstrated that environmental variables, such as [Cl^-] and pH, did not have a significant influence on the passive corrosion rate of Ti.[6,28–30] Thus, direct comparison of the passive dissolution rates on Ti Grade 2 in 1 M Cl^- and Ti Grade 7 in 5 M Cl^- can be made. Little difference between the passive corrosion rate of these materials was observed, with an average dissolution rate of 0.099 $\mu A/cm^2$ (or $8.6x10^{-4}$ mm/y) for Ti Grade 2 and 0.074 $\mu A/cm^2$ ($6.4x10^{-4}$ mm/y) for Ti Grade 7. The exact nature of the periodic fluctuations in the measured current are unclear; however, the values being measured are near the resolution limit of the instrument used. Thus, it is evident that Pd does not play a significant role in determining the passive corrosion rate of Ti. The most likely explanation for this is that Pd does not alter the anodic dissolution curve but simply alters cathodic reaction kinetics. More specifically, Pd alters the HER reaction kinetics, as discussed above. Thus, in oxidizing conditions where the dominant cathodic reaction is not HER, Pd does not play a significant role in altering either the anodic dissolution curve or the cathodic kinetics, and thus little effect is observed.

This explanation that Pd does not play a role in determining the passive corrosion of Ti in oxidizing conditions is in line with the reported benefits of Pd in reducing environments. For example, Okazaki et al.,[23] Shida and Kitayama,[24] and Shimogori et al.[25] all report increases in the concentration of Pd in the passive film on Ti during corrosion, in some cases increasing by as much

as a factor of 5.[24] It was also noted that the Pd concentration in the passive film on Ti increased with increasing exposure to the solution, and concomitantly the Ti dissolution rate was observed to decrease.[25] It should be noted, however, that all these observations were based on exposures to high concentrations of HCl at elevated temperature, and it seems likely that the accumulation of Pd in the passive film is through rapid, active dissolution of Ti. The subsequent decrease in the corrosion rate over time is then easily explained in terms of the discussion provided above with regard to crevice corrosion of Ti Grade 7. Thus, it appears that in mildly oxidizing, near neutral Cl^- solutions Pd does not influence the passive corrosion of Ti.

The addition of 1 M F^- to 1 M Cl^- significantly altered the anodic behavior of Ti Grade 7 (Figure 7). On polarization from open circuit, an initial passive region was observed prior to a current increase similar to that which is associated with a breakdown potential for localized corrosion. Under all conditions studied, though, general dissolution of the specimens was observed. Thus, the current increase observed after the initial passive region in F^- solutions is not associated with localized corrosion. Rather, further increases in the potential for F^- solutions resulted in the attainment of a critical current density (peak current density) after which increases in the potential resulted in decreases in the current density, similar to an active/passive transition. A peak current density of approximately 0.1 A/cm^2 was observed in all solutions with the potential-independent current density at higher potentials ranging from 10^{-3} to 0.1 A/cm^2, irrespective of material. These potential-independent currents were considerably higher than the passive current density observed in chloride-only solutions. Furthermore, given the magnitude of these currents, this region likely is not truly passive. It is possible that these high current densities are limited by transport of TiF_6^{2-} through a porous corrosion layer on the surface, similar to the mass transport conditions encountered

in electropolishing. Another possibility, which has been proposed in the literature for this apparent mass transport limited dissolution region,[31–33] is the transport of HF to the metal surface as a rate determining step in the reaction sequence shown in Eq. 7,

$$Ti^{4+}_{\text{passive film}} + 2HF \rightarrow TiF_2^{2+} + 2H^+ \quad (7)$$

Thus, it is clear that the presence of F^- resulted in marked changes in the anodic behavior and dissolution rate, basically shifting the anodic dissolution curve to higher currents, thereby also decreasing the open circuit potential.

Examination of the effect of $[F^-]$ on the dissolution rate at 0 V_{SCE} from long-term potentiostatic tests (Figures 8 and 9) indicate that a critical $[F^-]$ existed, above which a significant increase in dissolution rate was observed. This critical $[F^-]$ was ~ 0.5 mM. The existence of a critical $[F^-]$ is in line with what has been observed by others in other short term tests. Boere,[34] for example, observed a decrease in the polarization resistance of CP-Ti (similar to Ti Grade 2) in 0.2 M NaCl by a factor of over 30 when the $[F^-]$ was increased from 10 mM to 30 mM, in reasonable agreement with the observed increase by a factor of 7 for Ti Grade 2 at $[F^-]$ above 50 mM.

Given that Pd does not seem to influence the passive corrosion rate in Cl^- solutions nor does it seem to mitigate the detrimental effects of F^-, it would appear that the only role that Pd plays as an alloying element is by altering the cathodic reaction kinetics thereby increasing the resistance of Ti to localized corrosion. If only cathodic kinetics are affected, then one would not expect a change in the passive current density in Cl^- solutions, but open circuit potential would be expected to change. In air-saturated conditions (as would be expected in the proposed repository), little or no effect on the open circuit potential would be expected as the dominant cathodic reactant under most

conditions would be O_2, and Pd does not appear to alter the oxygen reduction reaction. Because F^- shifts the anodic dissolution curve to higher currents and promotes active dissolution by forming TiF_6^{2-} which is more stable than TiO_2, Pd likely does not alter this in any foreseeable way. Given the shift in open circuit to lower potentials with the shift in the anodic curve, however, Pd may play a small role in decreasing the open circuit potential. Anodic polarization by the presence of oxidizing species (e.g., Fe^{3+}, H_2O_2), however, would alter that behavior and any beneficial effects of Pd would likely be lost. Furthermore, the effect of other anionic species that have been observed to act as localized corrosion inhibitors in Cl^- solutions had little or not effect on the dissolution rate of Ti in the presence of F^-.

SUMMARY AND CONCLUSIONS

- Pd additions resulted in increasing E_{pit} and E_{rp} and appeared to convey immunity to crevice corrosion in Cl^- solutions but did not alter the passive dissolution rate in mildly oxidizing Cl^- solutions
- Importantly, Pd did not mitigate the deleterious effects of F^- on the anodic behavior of Ti
- Based on work conducted to date, the following mechanism is proposed:

    1. Addition of Pd to Ti results in increasing the exchange current density and decreasing the Tafel slope for the hydrogen evolution reaction
    2. Such changes raise the potential required to achieve sufficient Ti dissolution in pit embryos to sustain hydrolysis and attain the critical pH for pit propagation and also explain the immunity of Ti Grade 7 to crevice corrosion
    3. These changes to the hydrogen evolution reaction would not be expected to

significantly alter the passive current density in mildly oxidizing solutions as the primary governing cathodic reaction would not be hydrogen evolution.

4. Because F^- appears to alter anodic dissolution kinetics, Pd does not significantly mitigate this effect.

ACKNOWLEDGMENTS

The authors would like to acknowledge the financial support of the U.S. Nuclear Regulatory Commission (NRC), Office of Nuclear Material Safety and Safeguards, Division of Waste Management under contract No. NRC-02-97-009 in performing this work. The views presented herein are an independent product of the Center for Nuclear Waste Regulatory Analyses and do not necessarily reflect the regulatory position of the NRC. Technical assistance provided by Mr. S. Clay and Mr. J. Spencer (Southwest Research Institute) for some of the experimental work and SEM microscopy is gratefully acknowledged.

REFERENCES

1. Civilian Radioactive Waste Management System, Management and Operating Contractor, Repository Safety Strategy: Plan to Prepare the Postclosure Safety Case to Support Yucca Mountain Site Recommendation and Licensing Considerations, TDR-WIS-/RL-000001, rev 3, Las Vegas, NV: TRW Environmental Safety Systems, Inc. (2000).

2. Civilian Radioactive Waste Management System, Management and Operating Contractor, Waste Package Degradation Process Model Report, TDR–WIS–MD–000002, Revision 00 ICN 01, Las Vegas, NV: TRW Environmental Safety Systems, Inc. (2000).

3. D.W. Shoesmith, Review Of The Expected Behavior Of Alpha Titanium Alloys Under Yucca Mountain Conditions, AECL-12089, TDR - MGR-SE-000002 Rev.00, Pinawa, Manitoba: Atomic Energy Canada Limited (2000).

4. G.A. Cragnolino, D.S. Dunn, C.S. Brossia, J. Jain, and K.S. Chan. Assessment of Performance Issues Related to Alternate Engineered Barrier System Materials and Design Options, CNWRA 99-003, San Antonio, TX: Center for Nuclear Waste Regulatory Analyses (1999).

5. C.S. Brossia and G.A. Cragnolino, Effects of Environmental, Electrochemical, and Metallurgical Variables on the Passive and Localized Dissolution of Ti Grade 7, CORROSION 2000, Paper no. 211, Houston, TX: NACE International (2000).

6. C.S. Brossia and G.A. Cragnolino, Corrosion, 57, 768 (2001).

7. H. Satoh, K. Shimogori, and F. Kamikubo, Platinum Metals Review, 31, 115 (1987).

8. R.W. Schutz and M. Xiao, in Corrosion Control for Low-Cost Reliability, Proceedings 12th International Corrosion Congress, 1213, NACE International (1993).

9. P. McKay in Corrosion Chemistry within Pits, Crevice and Cracks, A. Turnbull, editor, London, England: Her Majesty's Stationary Office (1984).

10. B.M, Ikeda, M.G. Bailey, D.C. Cann, and D.W. Shoesmith in Advances in Localized Corrosion, NACE–9, H. Isaacs, U. Bertocci, J. Kruger, and S. Smialowska, editors, Houston, TX: NACE International (1987).

11. C.S. Brossia and G.A. Cragnolino, Effect of Palladium on the Localized and Passive Dissolution of Titanium, CORROSION 2001, Paper no. 01127, Houston, TX: NACE International (2001).

12. T.R. Beck, in Localized Corrosion, NACE-3, 644, Houston, TX: NACE International (1974).

13. T. Koizuka and S. Furuya, Titanium Science and Technology, Vol. 4, Plenum Press, New York, NY, p. 2383, (1973).

14. F.A. Posey and E.G. Bohlmann, Desalination 3: 269-279 (1967).

15. R.W. Schutz, in Corrosion Tests and Standards: Application and Interpretation, p. 493, West Conshohocken, PA: ASTM (1995).

16. F.A. Cotton and G. Wilkinson, Advanced Inorganic Chemistry, New York, NY: John Wiley & Sons (1980).

17. J.R. Galvele, in Treatise on Materials Science and Technology, vol. 23, 1, J.C. Scully Ed., New York, NY: Academic Press (1983).

18. J.B. Cotton, in Localized Corrosion, NACE-3, 676, Houston, TX: NACE International (1974).

19. J.O'M. Bockris and A.K.N. Reddy, Modern Electrochemistry, New York, NY: Plenum Press (1970).

20. E. Gileadi, Electrode Kinetics for Chemists, Chemical Engineers, and Materials Scientists, New York, NY: VCH Publishers (1993).

21. N.D. Tomashov, G.P. Chernova, V.N. Modestova, T.V. Chukalovskaya, L.N. Volkov, and R.P. Vasilyeva, in 4th International Congress on Metallic Corrosion, 642, Houston, TX: NACE International (1972).

22. T. Fukuzuka, K. Shimogori, and H. Satoh, in Titanium Science and Technology, 2695, Warrendale, PA: AIME (1980).

23. Y. Okazaki, K. Kyo, Y. Ito, and T. Tateishi, Materials Transactions, 38, 344 (1997).

24. Y. Shida and S. Kitayama, in 6th World Conference on Titanium, 1729 (1988).

25. K. Shimogori, H. Sato, H. Tomari, and A. Ooki, in Titanium and Titanium Alloys, vol. 2, 881, J.C. Williams and A.F. Belov Eds., New York, NY: Plenum Press (1976).

26. R.W. Schutz and J.S. Grauman, Laboratory corrosion behavior of titanium and other high performance alloys in representative FGD scrubber environments, Corrosion/85, Paper no. 52, Houston, TX: NACE International (1985).

27. W. Wilhelmsen and A.P. Grande, Electrochimica Acta, 32, 1469 (1987).

28. D.G. Kolman and J.R. Scully, Journal of the Electrochemical Society, 143, 1847 (1996).

29. D.G. Kolman and J.R. Scully, Journal of the Electrochemical Society, 141, 2633 (1994).

30. M. Conover, P. Ellis, and A. Curzon, in Geothermal Scaling and Corrosion, ASTM STP 717. Philadelphia, PA: American Society for Testing and Materials, 24 (1980).

31. M.J. Mandry and G. Rosenblatt, Journal of the Electrochemical Society, 119, 29 (1972).

32. V.A. Levin, Zashchita Metallov, 32, 143 (1996).

33. G.G. Kossyi, V.M. Novakovskii, and Ya.M. Kolotyrkin, Zashchita Metallov, 5, 210 (1969).

34. G. Boere, Journal of Applied Biomaterials, 6, 283 (1995).

TABLE 1

COMPOSITION OF TI GRADES 2 AND 7 USED IN THE CURRENT STUDY (WT%)

Material/Specimen	C	Fe	N	O	H	Pd	Ti
Grade 2 – cylindrical specimens	0.011	0.080	0.006	0.150	0.0015	–	bal.
Grade 2 – crevice specimens	0.032	0.080	0.002	0.110	0.0019	–	bal.
Grade 7 – all specimens	0.009	0.115	0.007	0.140	0.005	0.155	bal.

TABLE 2

PARAMETERS FOR EQ. 1 MEASURED IN THE PRESENT STUDY

Material	E^0_{pit} (V_{SCE})	B_{pit} (V/pCl^-)	E^0_{rp} (V_{SCE})	B_{rp} (V/pCl^-)
Ti Grade 7	7.69	2.00	5.61	1.02
Ti Grade 2, $[Cl^-] > 0.1$ M	1.08	1.30	0.72	1.06
Ti Grade 2, $[Cl^-] \leq 0.1$ M	4.26	1.83	3.11	1.77

Figure Captions

Figure 1: Effect of chloride concentration on the pitting (E_{pit}) and repassivation (E_{rp}) potentials for Ti Grades 2 and 7 in deaerated solutions at 95 °C.

Figure 2: SEM micrograph showing morphology of pitting attack after cyclic potentiodynamic polarization testing of Ti Grade 2 in deaerated 1 M NaCl at 95 °C.

Figure 3: Current density as a function of time for creviced Ti Grades 2 and 7 in 5 M chloride solutions and creviced Ti Grade 2 in 1 M chloride solution. All tests conducted under deaerated conditions at 0 V_{SCE} and 95 °C. Inset figure shows expanded view of passive currents measured.

Figure 4: SEM micrograph of crevice corrosion on Ti Grade 2 after polarization at 0 V_{SCE} in 1 M chloride at 95 °C.

Figure 5: Cathodic polarization curves for Ti Grades 2 and 7 in deaerated 5 M chloride + 0.1 M HCl at 95 °C. Dotted lines represent linear regression lines used to calculate cathodic Tafel slopes.

Figure 6: Anodic polarization curves for Ti Grades 2 and 7 in deaerated 5 M chloride + 0.1 M HCl at 95 °C.

Figure 7: Polarization curves for Ti Grade 7 in the presence and absence of 1 M fluoride under deaerated conditions at 95 °C.

Figure 8: Effect of fluoride concentration on the dissolution rate of Ti Grade 7 at a potential of 0 V_{SCE} over time (deaerated, 1 M NaCl at 95 °C).

Figure 9: Effect of fluoride concentration on the dissolution rate of Ti Grade 7 after potentiostatic polarization at 0 V_{SCE} for 453 hours (deaerated, 1 M NaCl at 95 °C).

Figure 10: Effect of other differing solution compositions some containing additional anionic species (i.e., nitrate and sulfate) on the dissolution rate of Ti Grade 7 at a potential of 0 V_{SCE} over time

(deaerated solutions at 95 °C).

Figure 11: Open circuit potentials measured under air-saturated conditions at 95 °C.

Figure 12: SEM micrograph of corrosion attack observed under the crevice former for Ti Grade 7 in deaerated 1 M NaCl at 95 °C after polarization at an applied potential of 7 V_{SCE} for 28 hours.

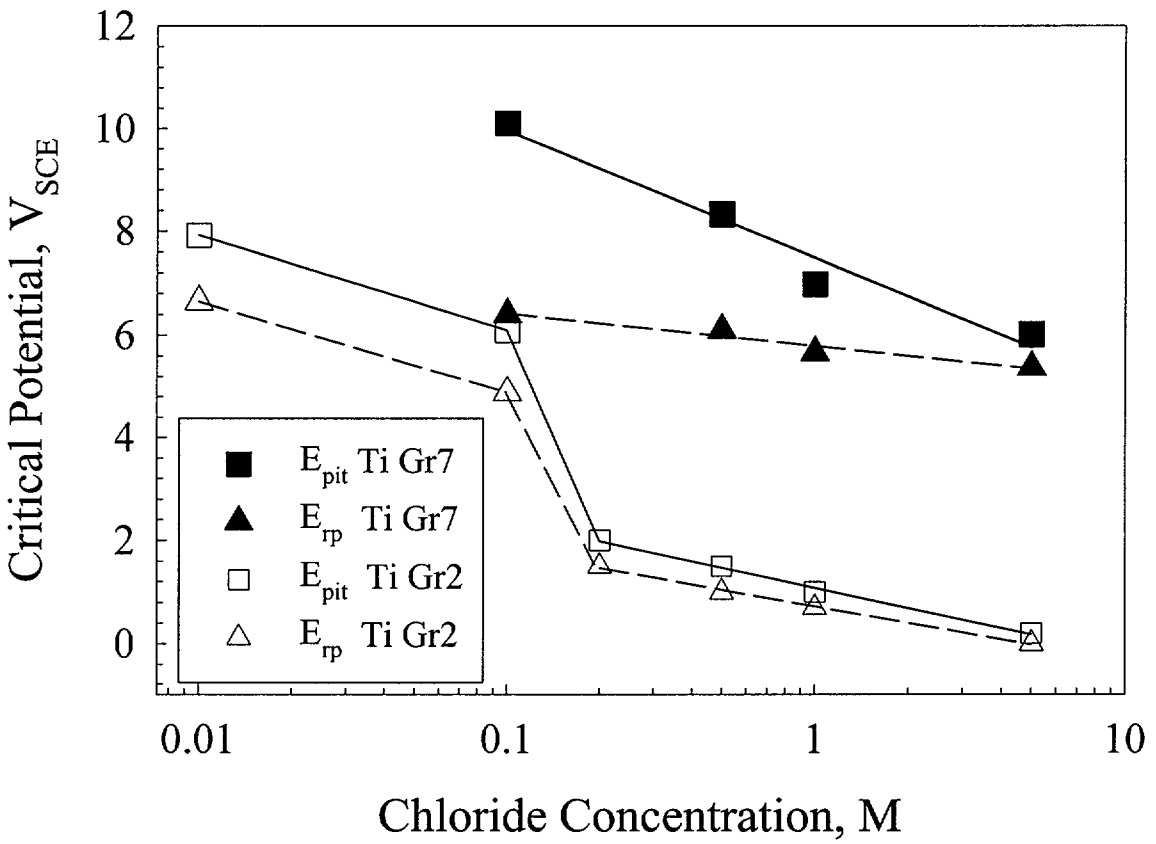
12
10
8
6
4
2
0
Critical Potential, V_{SCE}
E_{pit} Ti Gr7
E_{rp} Ti Gr7
E_{pit} Ti Gr2
E_{rp} Ti Gr2
0.01
0.1
1
10
Chloride Concentration, M

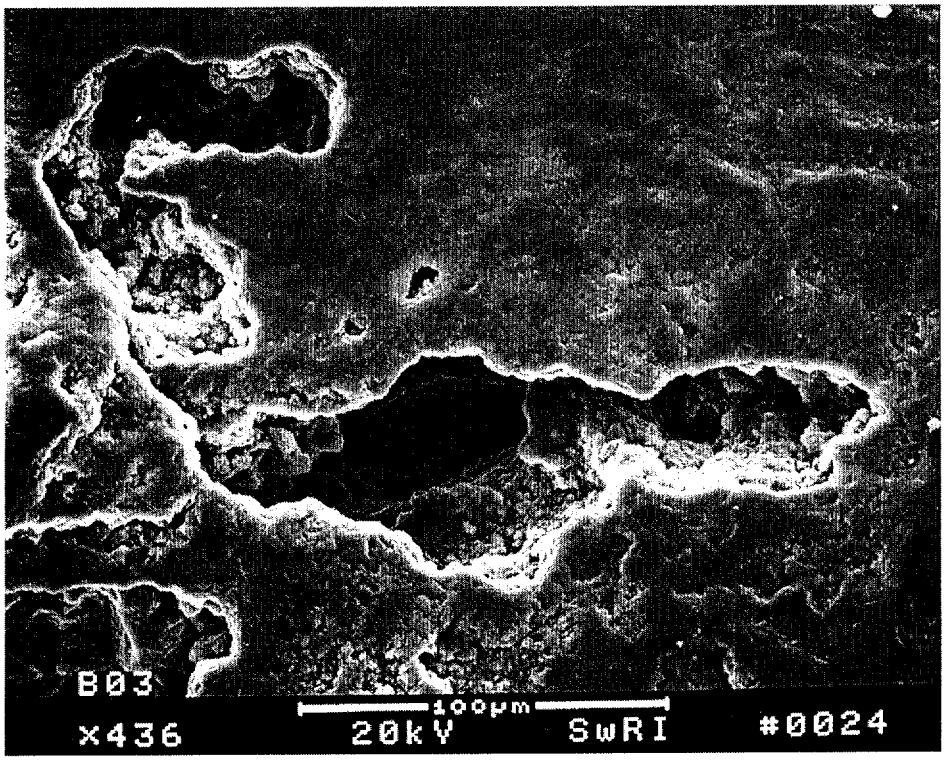

2

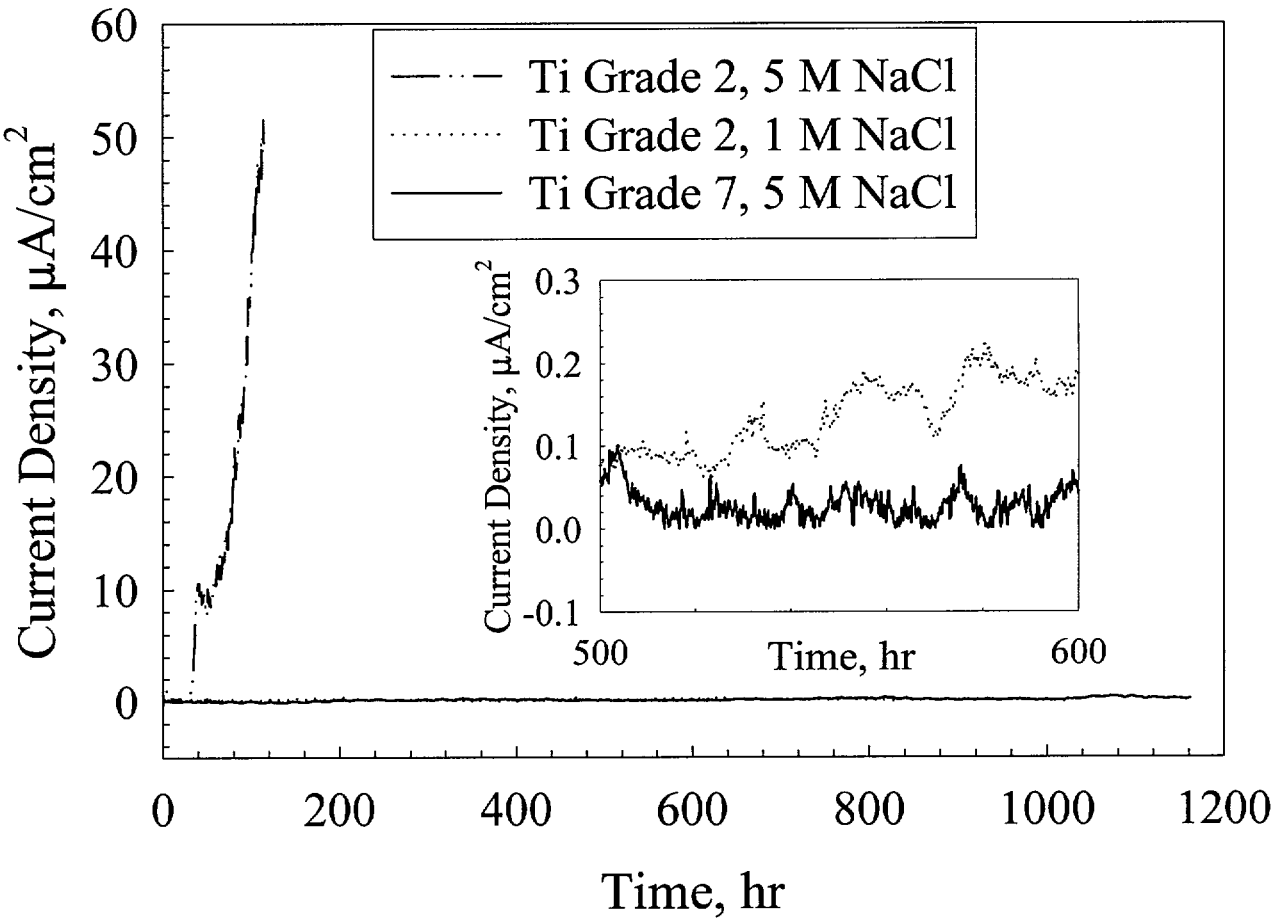
Ti Grade 2, 5 M NaCl
Ti Grade 2, 1 M NaCl
Ti Grade 7, 5 M NaCl
Current Density, μA/cm2
Time, hr
0
10
20
30
40
50
60
0
200
400
600
800
1000
1200
Current Density, μA/cm2
0.3
0.2
0.1
0.0
-0.1
500
600
Time, hr

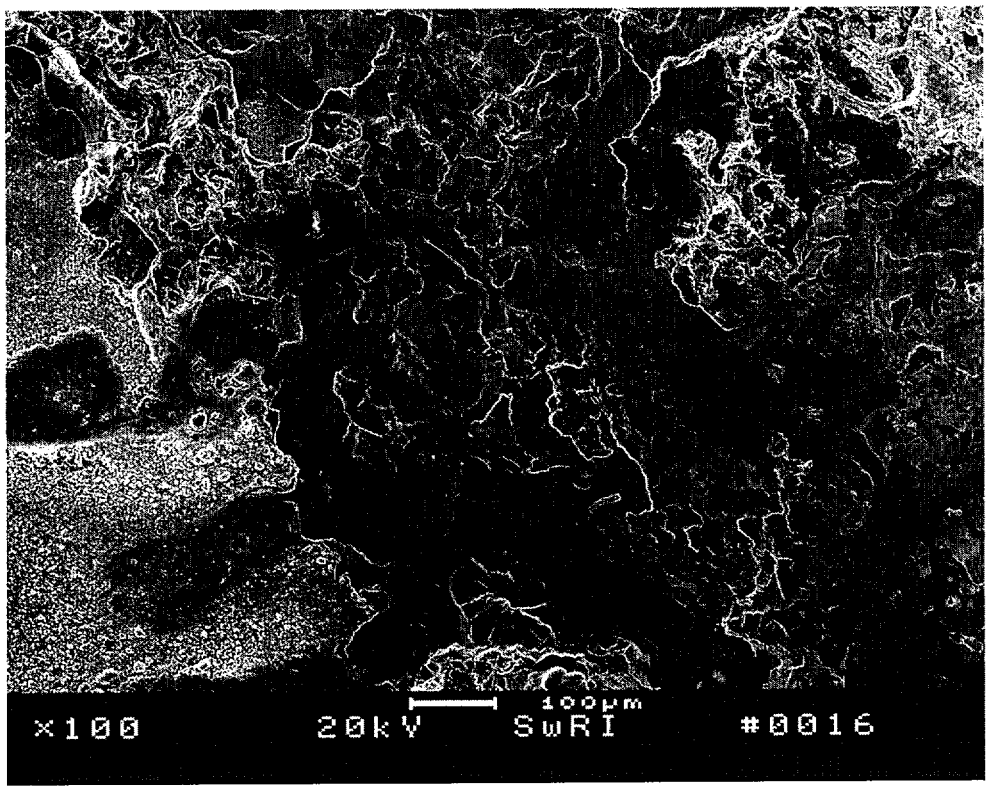
100μm
×100
20kV
SwRI
#0016

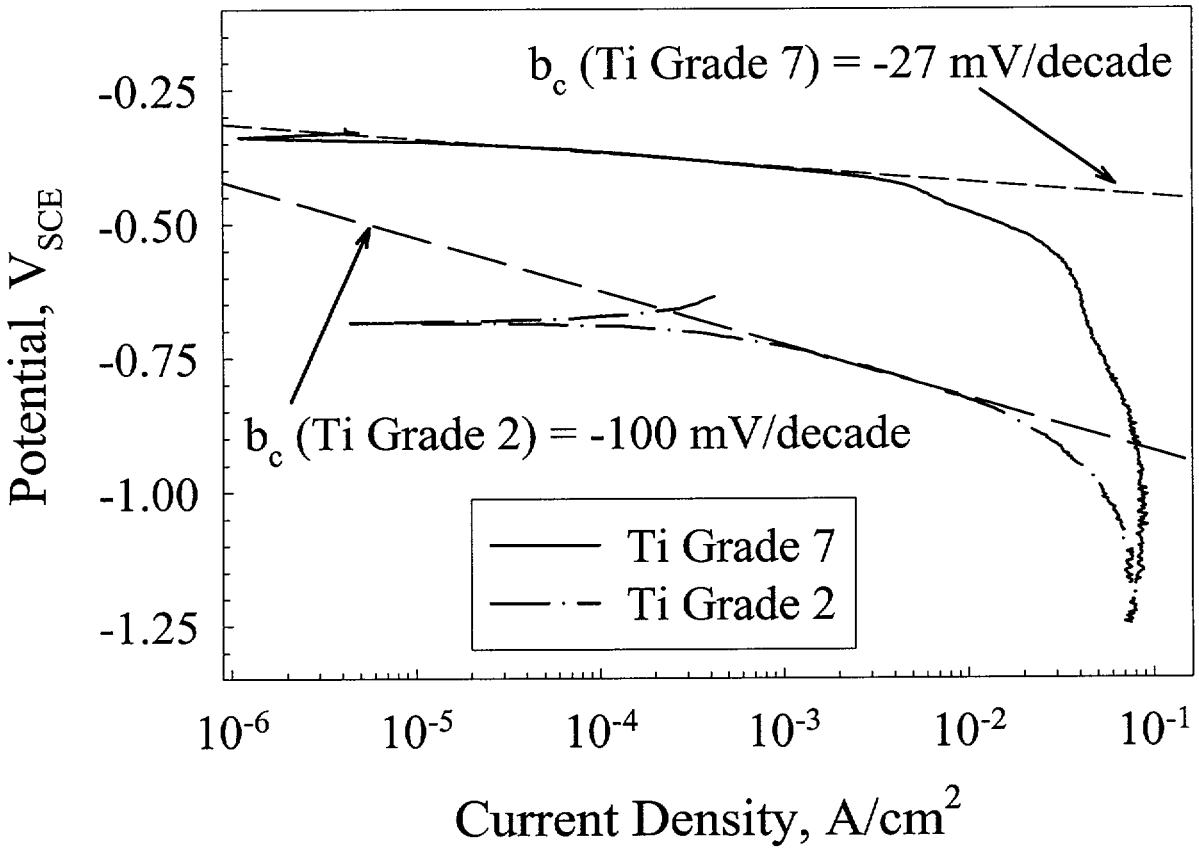
b_c (Ti Grade 7) = -27 mV/decade
b_c (Ti Grade 2) = -100 mV/decade
Ti Grade 7
Ti Grade 2
-0.25
-0.50
-0.75
-1.00
-1.25
Potential, V_SCE
10^-6
10^-5
10^-4
10^-3
10^-2
10^-1
Current Density, A/cm^2

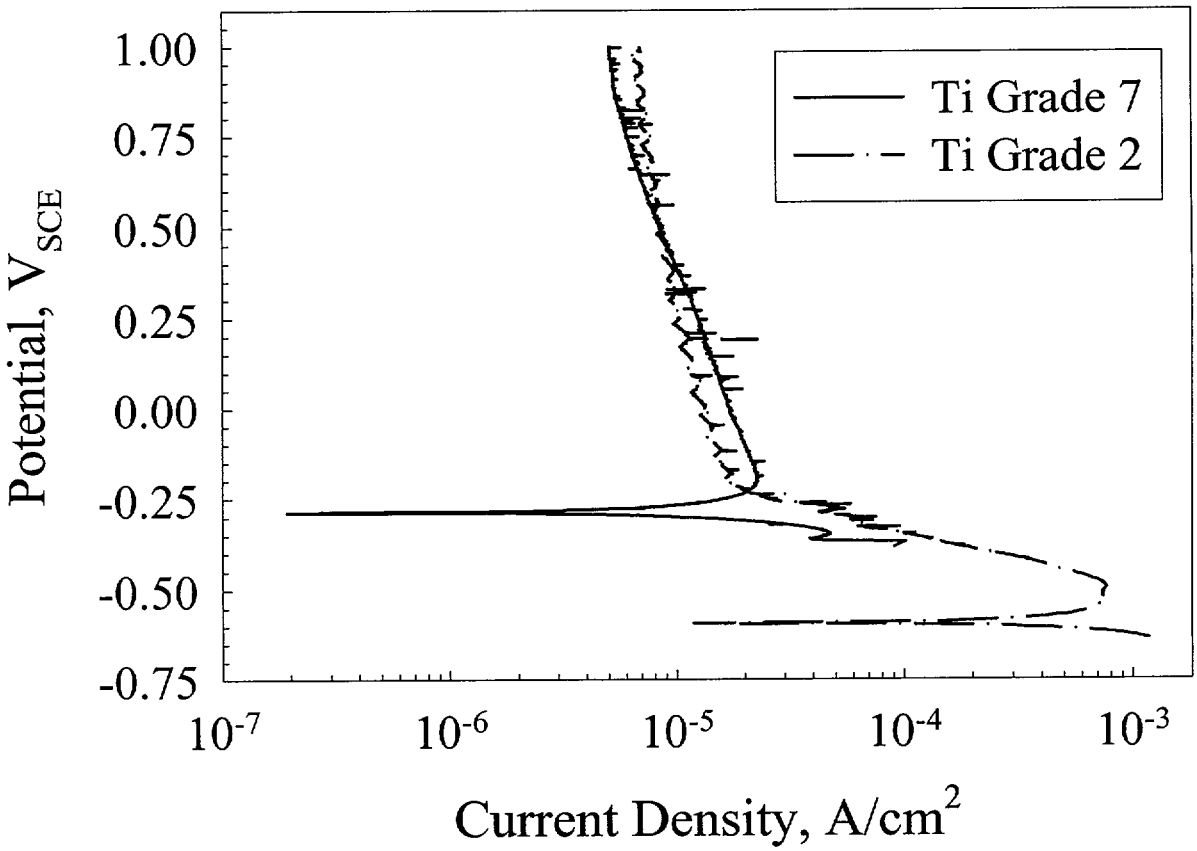
1.00
0.75
0.50
0.25
0.00
-0.25
-0.50
-0.75
Potential, V_{SCE}
10^{-7}
10^{-6}
10^{-5}
10^{-4}
10^{-3}
Current Density, A/cm^2
Ti Grade 7
Ti Grade 2

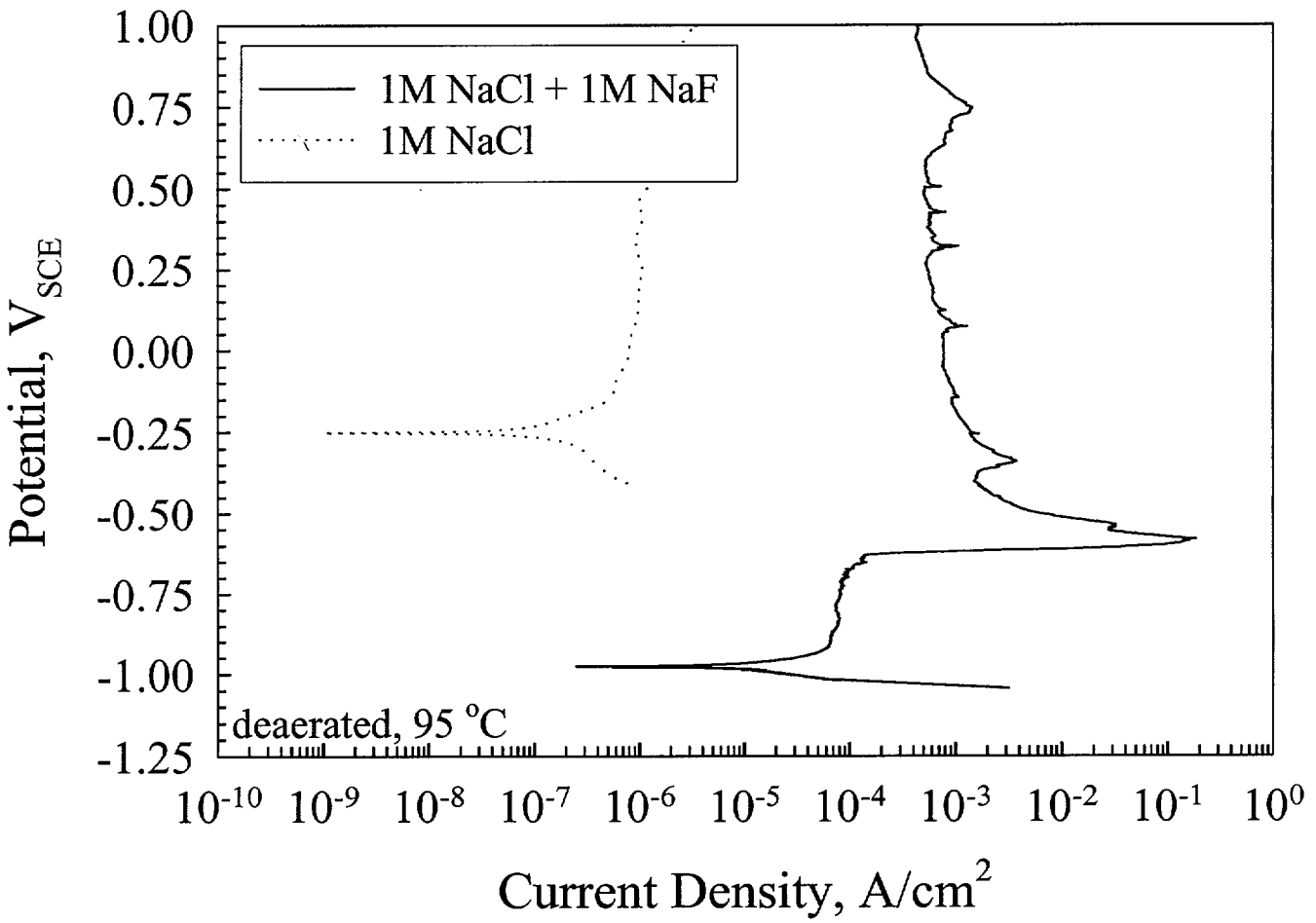
1.00
0.75
0.50
0.25
0.00
-0.25
-0.50
-0.75
-1.00
-1.25
Potential, V_{SCE}
1M NaCl + 1M NaF
1M NaCl
deaerated, 95 °C
10^{-10} 10^{-9} 10^{-8} 10^{-7} 10^{-6} 10^{-5} 10^{-4} 10^{-3} 10^{-2} 10^{-1} 10^{0}
Current Density, A/cm^2

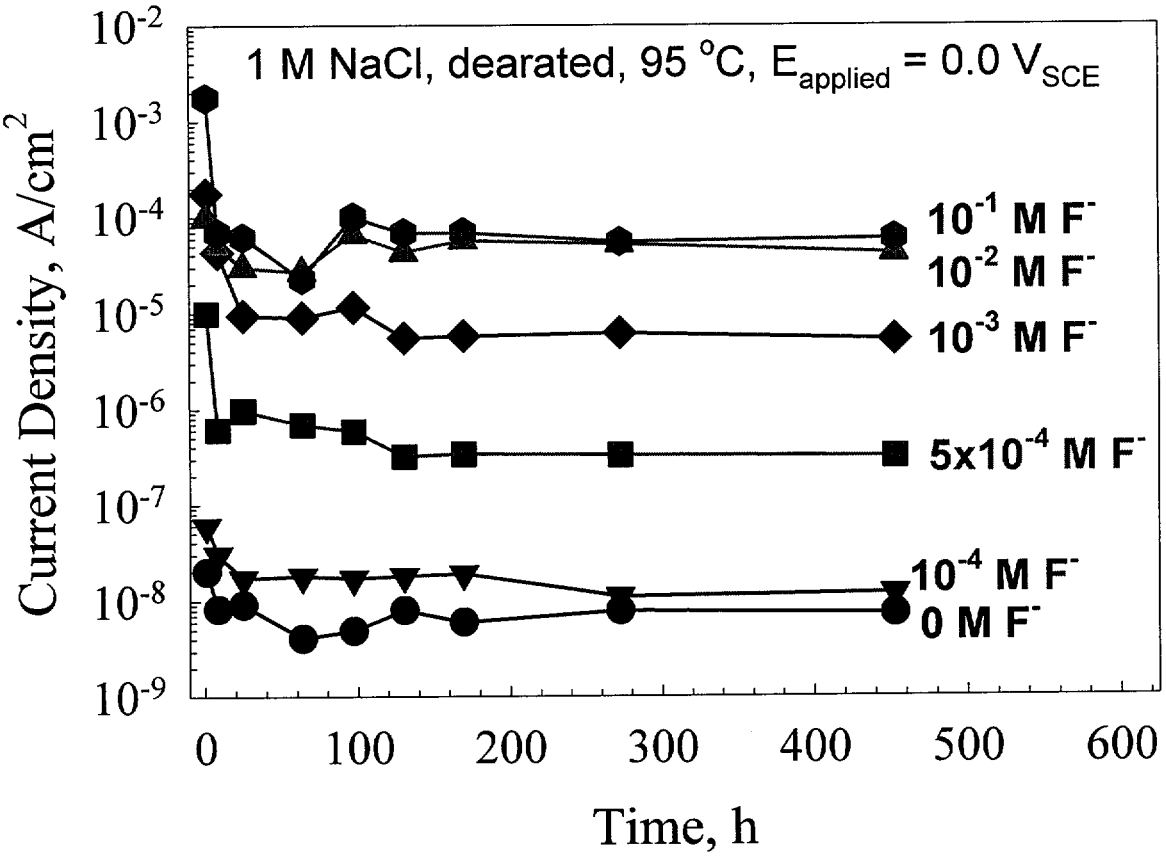
1 M NaCl, dearated, 95 °C, E applied = 0.0 V SCE
Current Density, A/cm2
10-2
10-3
10-4
10-5
10-6
10-7
10-8
10-9
0
100
200
300
400
500
600
Time, h
10-1 M F-
10-2 M F-
10-3 M F-
5x10-4 M F-
10-4 M F-
0 M F-

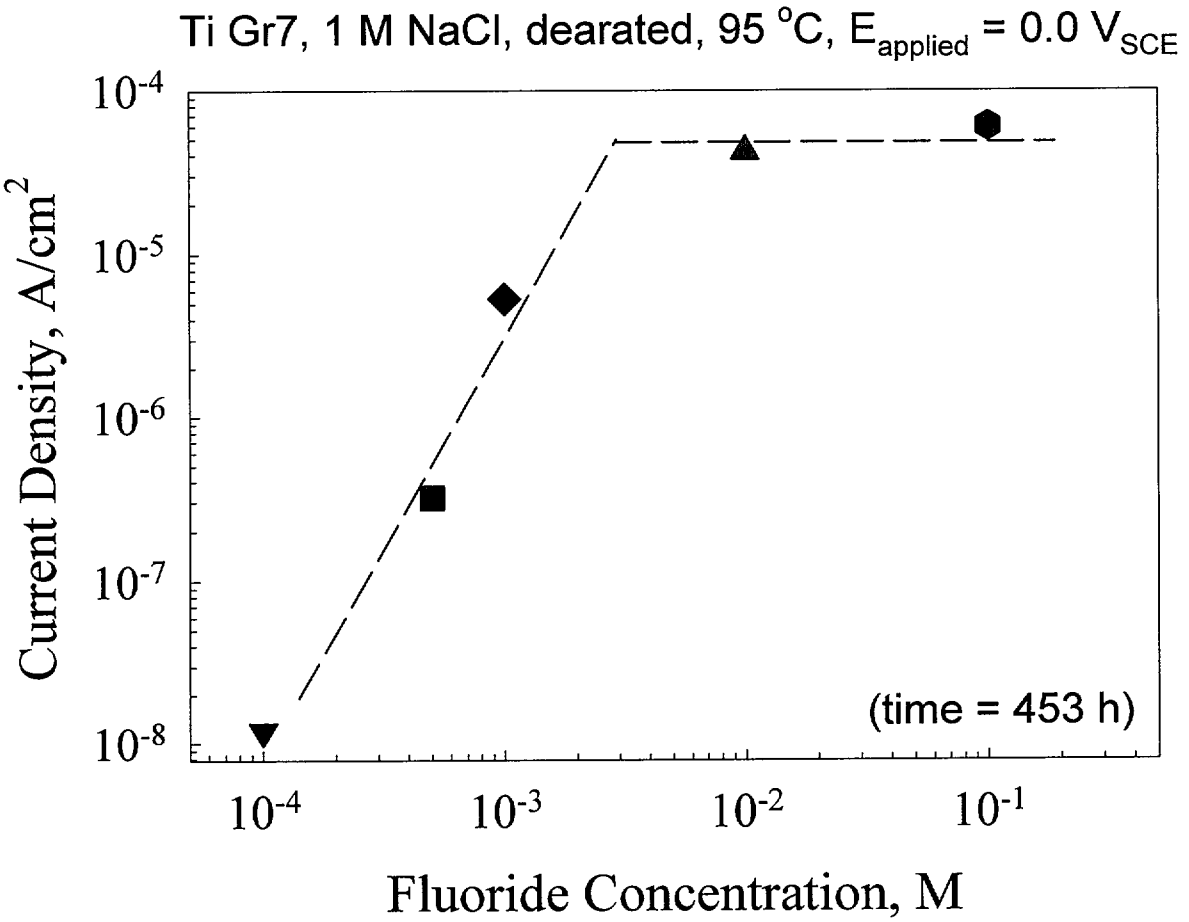
Ti Gr7, 1 M NaCl, dearated, 95 °C, E applied = 0.0 V SCE
Current Density, A/cm2
10-4
10-5
10-6
10-7
10-8
(time = 453 h)
10-4
10-3
10-2
10-1
Fluoride Concentration, M

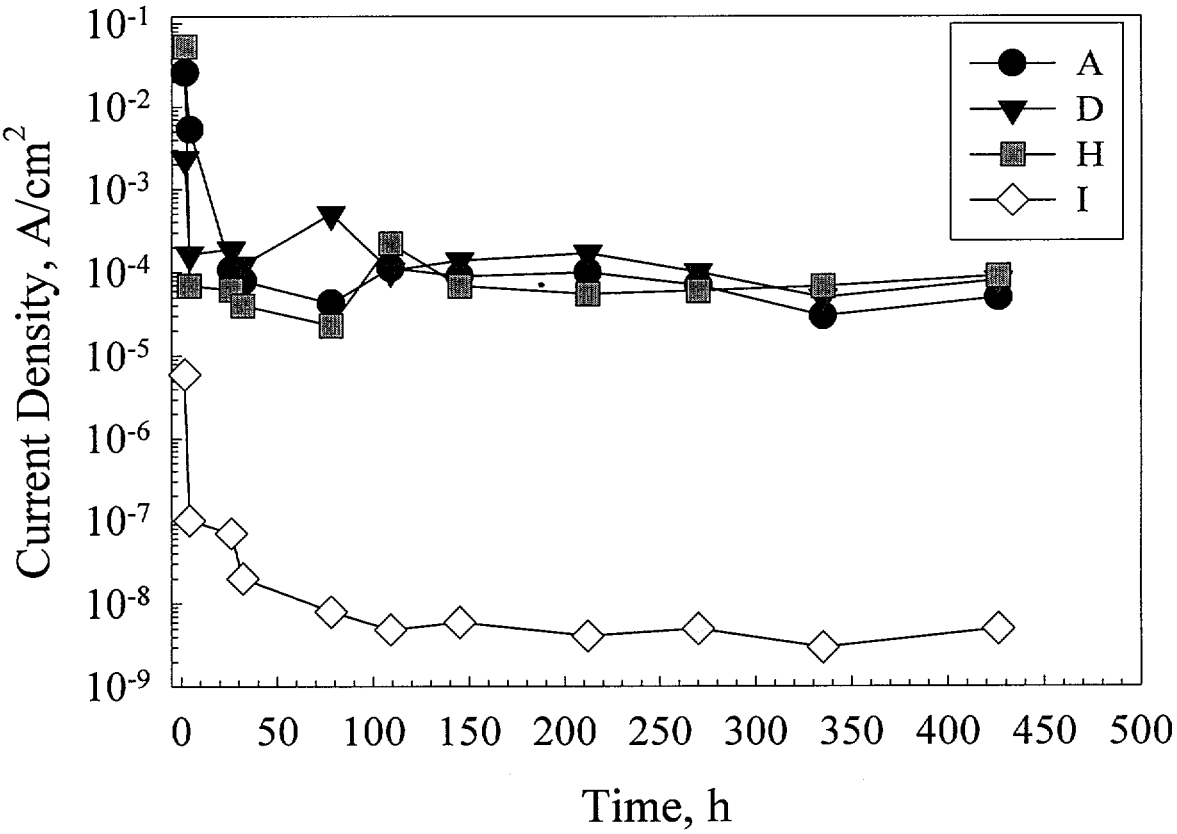

A = 1 M Cl^-, 0.1 M F^-, 0.55 M NO_3^-, 0.92 M SO_4^{2-}
D = 3.84 M Cl^-, 0.07 M F^-, 2.32 M NO_3^-, 0.15 M SO_4^{2-}
H = 1 M Cl^-, 0.1 M F^-, 0.0 M NO_3^-, 0.0 M SO_4^{2-}
I = 1 M Cl^-, 0.0 M F^-, 0.0 M NO_3^-, 0.0 M SO_4^{2-}.

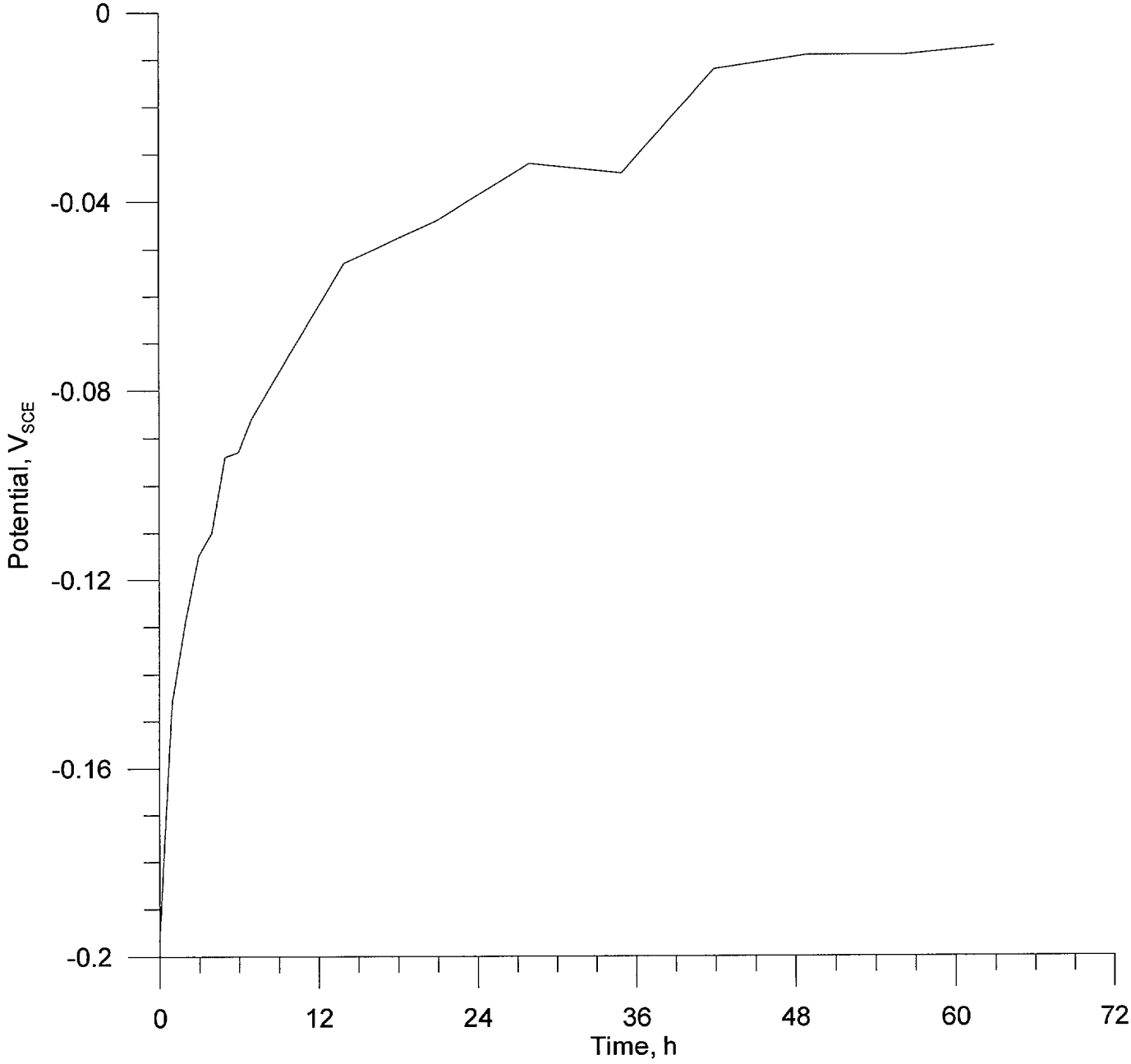

11

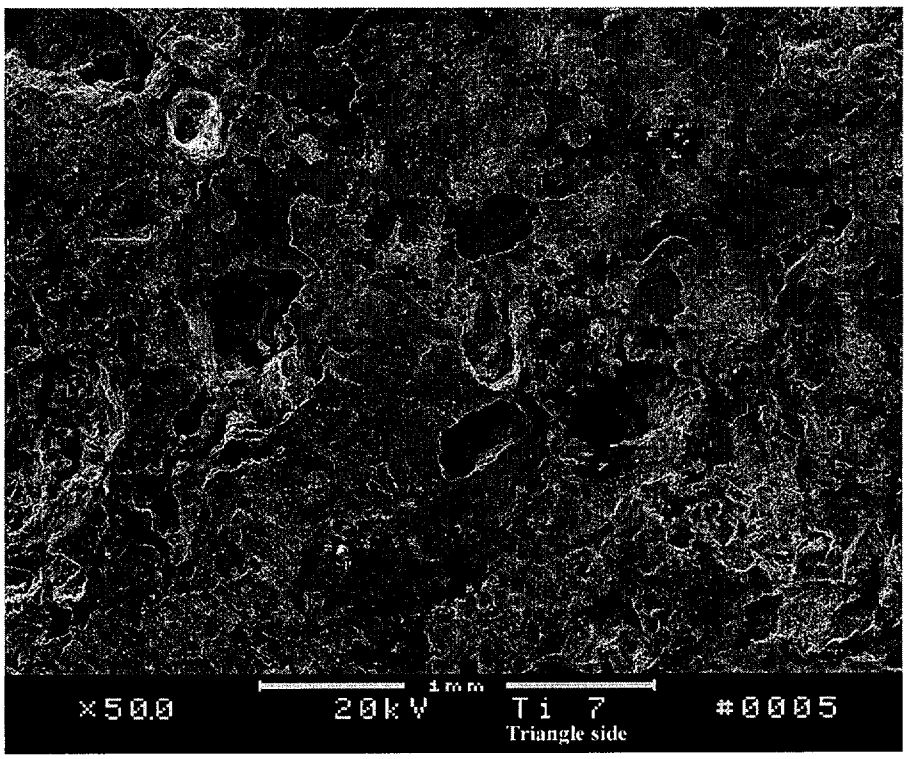
1mm
×50.0
20kV
Ti 7
#0005
Triangle side